Smart Operation of Electric Vehicles with Four-Quadrant Chargers Considering Uncertainties

Nafeesa Mehboob, *Member, IEEE*, Mauricio Restrepo, *Student Member, IEEE*, Claudio A. Cañizares, *Fellow, IEEE*, Catherine Rosenberg, *Fellow, IEEE*, Mehrdad Kazerani, *Senior Member, IEEE*

Abstract—Given the expected impact of electric vehicle (EV) charging on power grids, this paper presents a novel two-step approach for the smart operation of EVs with four-quadrant chargers in a primary distribution feeder, accounting for the uncertainties associated with EVs, and considering the perspectives of both the utility and the EV owners. In the first step of the proposed approach, the mean daily feeder peak demand and corresponding hourly feeder control schedules, such as taps and switched capacitor setpoints, considering the bidirectional active and reactive power transactions between EVs and the grid, are determined. A nonparametric Bootstrap technique is used, in conjunction with a genetic algorithm (GA)-based optimization model, to account for EV uncertainties and discrete variables. In the second step, the maximum possible power that can be given to connected EVs at each node, while providing active and/or reactive power to maintain the peak demand value and corresponding feeder dispatch schedules defined in the first step, is computed every few minutes in a way which is fair to the EVs. The proposed approach is validated using the distribution feeder model of a real primary feeder in Ontario, Canada, considering significant EV penetration levels. The results show that the proposed approach could be implemented in practice to properly operate EVs, satisfying feeder and peak demand constraints, which would be better than the business-as-usual practice or a popular heuristic method in terms of number of tap operations, system peak demand, and voltage regulation.

Index Terms—Bootstrap, distribution system management, electric vehicle, EV smart charging, uncertainty, vehicle-to-grid.

NOMENCLATURE

Sub- and Super-Indices

b	Feeder index
ev	Aggregated EV index
i	LTC tap index
j	Switched capacitor index
l	Vehicle index
n	Node index
pk	Peak
t	Time interval index

Parameters

$\bar{\ }, \underline{\ }$	Upper and lower limits
$\overline{cap}_j$	Upper limit for switched capacitor [kVAr]
$\overline{Eev}_n$	Battery capacity of aggregate EV load [kWh]
$\overline{SoC}_l$	SoC upper limit [%]
τ_1, τ_2	Time steps
AHD	Average hourly demand [kWh]
B	Number of feeders in the system
$BCap$	Battery capacity of single EV [kWh]
EVr	Electric range of EV [km]
K	Number of elements in the sample
LN	Number of load nodes in the system
M	Number of Bootstrap samples
Mcp	Maximum limit of single charging point [kW]
Mop	Maximum control operations per hour for taps (Mop_{tap}) and capacitors (Mop_{cap})
N	Total number of nodes in the system
nev	Number of EVs
pr	Penetration rate
SoC^f	SoC at the end of charging period [%]
T_{max}	Maximum time limit

Variables

α, β	Discharging control variables
δ_n	Voltage angle [rad]
$\hat{C}on$	Mean hourly feeder control schedule
$\hat{P}^{max}$	Mean daily feeder peak demand for original sample [kW]
$|V^{bc}|$	Base-case voltage magnitude [p.u.]
cap	Integer capacitor switch setting
$E[Con]$	Bootstrap estimate of hourly feeder control schedule
$E[P^{max}]$	Bootstrap estimate of daily feeder peak demand [kW]
EVd	Distance travelled by aggregate EV load [km]
I	Current phasor [p.u.]
J	Jacobian matrix
P	Active power demand [kW]
P^{max}	Daily feeder peak demand [kW]
Q	Reactive power demand [kVAr]
S	Apparent power phasor [kVA]
SoC	EV Battery SoC [%]
SoC^0	SoC at the beginning of charging period [%]
$T_n^{Arr,Dep}$	Arrival, departure time of aggregate EV load
tap	Integer tap setting
V	Voltage phasor [p.u.]
$BL_{n,t}$	Base load [kW]
$P^{ev+,-}$	Charging and discharging EV load [kW]

I. INTRODUCTION

DISTRIBUTION feeders are designed to serve forecasted loads, and not electric vehicle (EV) loads. Hence, the task of optimal operation of distribution feeders in this context is a complex problem, due to the significant increase in demand and the uncertainties associated with EV charging, when EV penetration is high [1]. Most of EVs arrive home and start charging at a time which coincides with the peak period of residential areas, which may lead to new peaks or an increase in peak demand in distribution feeders. Incentive programs to reduce the peak demand of the system and maximize the utilization of existing assets have been implemented by several utilities in North America (e.g. Peaksaver Plus® program in Ontario [2]), as an increase in peak demand may require significant capital investment and infrastructure upgrades. Hence, on one hand, utilities are concerned with a higher system peak due to the charging of EVs if the penetration is high, while on the other hand, the customers want fast and fair charging; these are the problems this paper tries to address.

Several works in the literature address dynamic or real-time operation of EV loads in distribution systems using a centralized or decentralized approach. Many papers (e.g. [3], [4]) take the vehicle perspective only, ignoring the grid; hence, the practical feasibility of the proposed algorithms from a grid perspective is not analyzed or verified. The decentralized charging strategies proposed in [5] aim to schedule EV loads in real-time and in a fair manner, while taking the operational constraints of the grid into account; this charging strategy ensures fairness in the frequency at which EVs are allowed to charge from the grid, but not in terms of the energy they receive, and has a high communication overhead. The decentralized charging strategy proposed in [6] for real-time EV charging is fast and robust, but does not address the problem of tap and capacitor scheduling.

In [1] and [7]–[11], centralized strategies to charge EVs dynamically are proposed. In [7], a cost minimizing strategy benefitting the utility alone is proposed, neglecting fairness in charging for all EVs, while in [8], fair EV charging leads to an increase in system peak, which is not favourable to the utility. A joint optimal power flow (OPF) and EV charging approach is proposed in [9]; however, the uncertainties associated with EVs are not considered, which is an important factor in real-time charging of EVs. In [1], [10], and [11], the authors propose centralized control schemes, considering the uncertainty associated with EVs, but [10] only considers the stochasticity in arrival time of EVs, and the proposed priority-based charging scheme does not ensure fairness in charging. In [1] and [11], the dynamic nature of the EVs is considered while maximizing the power given to EVs, but simplified distribution grid models are used to reduce computational burden.

Four-quadrant chargers allow EVs to inject or absorb active and/or reactive power, enabling operation in vehicle-to-grid (V2G) mode and thus, adding more control options for distribution feeders. The operation of four-quadrant EV chargers in distribution feeders has been considered in several works, such as [12]–[14], which have mostly focused on reactive power control with EVs to improve voltage profiles and minimize losses without discharging EV batteries. Thus, [12] considers the simultaneous operation of four-quadrant EV chargers, load tap changers (LTCs), and switched capacitors for minimization of losses and capacitor operation costs; however, the inductive and discharging regions of EV chargers are not studied; also, the uncertainties of EV operation are not included. In [13], a robust multi-objective optimization model for both minimizing charging costs and voltage deviations using four-quadrant EV chargers, including the uncertainties of EV operation, is presented; however, this approach does not consider battery discharging, nor distribution feeder LTCs and switched capacitors, given the linear nature of the robust formulation. In [14], a similar approach to the one discussed in the current paper is proposed; however, only two-quadrant operation is considered, and the impact of different penetration levels are not analyzed. There are various papers that discuss schemes and procedures (e.g. [15]) to compensate EVs for reactive and active power services, which are beyond the scope of the present paper, since it focuses on the optimal operation of four-quadrant EV chargers in primary distribution feeders; however, the approach proposed here could be used to design possible compensation methods for EV P and Q distribution feeder services.

Based on the previous discussions, the present paper proposes a novel two-step approach for the smart operation of four-quadrant EV chargers in a primary distribution feeder, while considering the uncertainties associated with EVs, from the perspectives of both the utility and the customers, as well as the interactions with LTCs and switched capacitors, analyzing various operation modes of four-quadrant EV chargers. Thus, the main contributions of this paper are as follows:

- Proposing a new method to obtain day-ahead hourly feeder control schedules using an accurate and realistic model of a 3-phase unbalanced feeder, considering EV uncertainties, through a non-parametric Bootstrap technique, and operation in all the four quadrants of the PQ plane.
- Proposing a novel method for maximum possible power allocation to charge EV batteries using a proportional fairness approach, considering also the provision of active and reactive power from EV loads to support the grid, without exceeding a given peak demand setpoint or the feeder operational limits.
- Illustrating the benefits and feasibility of the proposed two-step approach for practical applications and feeder operation, based on the results obtained for an actual primary distribution feeder and realistic assumptions regarding several four-quadrant EV operation modes and uncertainties.

The rest of the paper is organized as follows: Section II presents background information about four-quadrant EV chargers. Section III describes the problem formulation of the proposed two-step approach. The first step of the proposed approach, i.e. the day-head dispatch of distributions feeders with four-quadrant EV chargers, is explained in Section IV. Section V presents the second step of the proposed approach,
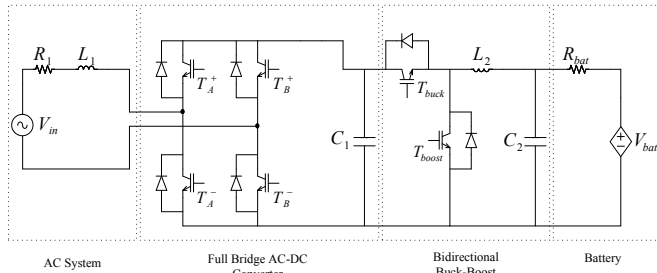
Fig. 1. Typical two-stage smart charger topology [18].

Fig. 2. Schematic overview of the proposed approach.

i.e. the fair charging of EV batteries, and the use of active and reactive power from EVs to support grid operation. A simpler heuristic approach and the business-as-usual (BAU) practice are used as benchmarks against which the performance of the proposed approach is evaluated in Section VI, where the test feeder used, the assumptions made, and the simulation results are presented and discussed. Finally, Section VI highlights the main conclusions and contributions from this work.

II. FOUR-QUADRANT EV CHARGERS

Four-quadrant EV chargers refer to a category of chargers that are able to operate at in all four quadrants of the PQ plane, particularly due to bidirectional power flow capability of the converters used, and independent and bidirectional reactive power control at the interface with the grid. In contrast with the existing EV chargers that are normally composed of a diode bridge rectifier and a boost converter for power factor correction, these chargers typically use a two-stage converter topology, with controllable switches, as shown in Fig. 1. The first stage is a single-phase, bidirectional, half-bridge or full-bridge ac/dc converter that is in charge of regulating the dc-link capacitor voltage and controlling the reactive power or power factor at the interface with the grid. The second stage is a bidirectional dc/dc converter, such as bidirectional buck-boost converter, that controls the battery current according to the charging or discharging set points [16]. In addition to being able to charge and discharge the EV battery, four-quadrant EV chargers allow injection and absorption of reactive power at the grid interface independently of the EV battery power, and merely based on the support of the dc-link capacitor, thus avoiding added stress on EV battery and dc/dc converter. The main disadvantage of four-quadrant chargers is the extra cost of converters [17].

Even though four-quadrant EV chargers are still not available in the EV models on the market, the technical feasibility of these chargers has been demonstrated with various prototypes for a wide range of active and reactive power set points (e.g. [18], [19]). Hence, the flexibility of EV loads equipped with four-quadrant chargers is an advantage that can be used by utilities to ensure efficient feeder operation through coordinated operation of EV loads and proper feeder management, while accounting for EV uncertainties, such as arrival and departure times, initial battery state of charge (SoC), and number of EVs charging [20]. Thus, this work proposes an approach to operate the distribution feeders efficiently when the
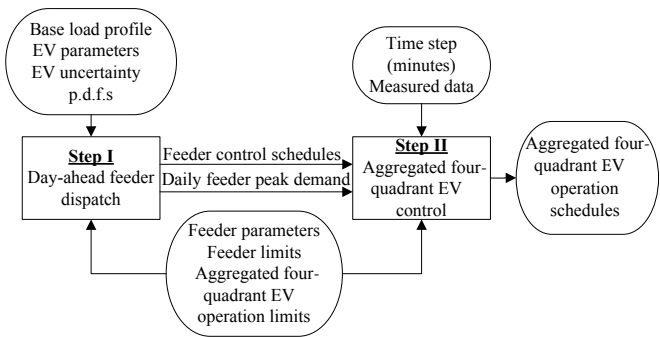
penetration of EVs with four-quadrant chargers is significant, while keeping the daily feeder peak demand reasonable. The proposed technique includes day-ahead dispatch of distribution feeders and quasi-real-time operation of four-quadrant EV chargers via centralized scheduling.

III. PROBLEM FORMULATION

A radial primary distribution feeder, with a specified number of nodes (bus and phase) and controllable LTCs and switched capacitors, is considered in this work. It is assumed that aggregated base and four-quadrant EV loads are present at each load node. Note that the present work deals with aggregated EV loads at each node, and hence does not deal with individual EV control, which requires the representation of the secondary distribution network, as discussed in [14], where the representation of the secondary distribution or low-voltage (LV) network for EV smart charging is studied in detail; in this paper, the dispatch of individual EV chargers may affect the active and reactive power set points, since the calculation of the final set points takes into account the ratings of the MV/LV distribution transformer, secondary feeder and service cables, as well as voltage limits at each LV node, which are not represented in aggregated load models. Furthermore, for simulation purposes, it is assumed that active and reactive powers at a load node are properly distributed among all EVs connected. It is also assumed that feeder controllable variables, i.e. tap and capacitor settings, can be adjusted every hour. The hourly base load profiles for each load node are assumed known through proper forecasting methods for a 24 h period (e.g. [21]), while EV loads, which are assumed controllable in smaller time steps (e.g. 5 min), are associated with temporal and spatial uncertainties, i.e. the arrival and departure times, and the initial SoCs at any given time at any node are random variables.

This work addresses the operation process in two steps, as shown in Fig. 2. First, the day-ahead dispatch of a distribution feeder is performed considering uncertainties in the arrival and departure times and the initial battery SoCs at each node as follows:

- *Arrival and Departure Times*: The aggregated arrival and departure times of four-quadrant EV loads at each node follow given probability distribution functions (pdfs), accounting for the temporal uncertainty of these loads,

thereby dictating the total time available to operate the EVs for a specific final battery SoC.

- *Initial Battery SoC*: The initial battery SoC of aggregate EV loads at node n is calculated using:

$$SoC_n^0 = \left(1 - \frac{EVd_n}{EVr}\right) 100 \quad \forall \, n = 1, ..., LN \quad (1)$$

based on the aggregated daily distance traveled by the electric vehicles EVd_n, which is a random variable following a given pdf, and the EVs' electric range EV_r. The variation in initial battery SoC affects the total energy drawn from the grid by the EVs.

The base load profiles, and aggregated EV and feeder parameters and limits, are inputs to the first step. In this step, hourly τ_1 tap and capacitor schedules, as well as the EV active and reactive power schedules, are computed for one day for various realizations of the above-mentioned uncertainties, to minimize daily feeder peak demand, while satisfying all feeder and EV-related constraints based on an optimization approach. These tap and capacitor schedules and daily feeder peak demand values are then used to compute a feeder control schedule that is likely to work well over a large number of realizations for a mean peak demand value. The feeder tap and capacitor schedule and peak demand are inputs to the second step, which performs aggregated four-quadrant EV control; aggregated EV operation limits, and feeder limits and parameters are also inputs to the second step. The output of the second step, which is computed every few minutes (τ_2=5 min) is the per-node aggregated EV active and reactive power for that period.

It is important to note that, in the first step, all the EVs at a node are assumed to be aggregated into one uncertain and variable load, so that uncertainties on EV arrival and departure times, as well as initial battery SoCs, are all represented through a combined stochastic load. Additionally, the quality of the stochastic representation of EV loads will depend on the quality of the data sets used to extract the pdfs; the pdfs used in this paper are extracted from [22] and [23]. However, the model proposed in this paper is independent of the EV data; thus, if other pdfs extracted from different EV data sets become available, they can be readily integrated into the model. On the other hand, in the second step, the stochasticity associated with each EV at a node, in terms of the arrival and departure times, and the initial battery SoCs, is considered using the same pdfs used in the first step, so that the number of EVs needed for simulation purposes can be computed for each time interval; in practice, this information would be available in real time through a communication network.

IV. DAY-AHEAD DISPATCH OF DISTRIBUTION FEEDERS WITH FOUR-QUADRANT EV CHARGERS

The objective of the first step is to compute a feeder control schedule that would allow for the operation of the grid within operating limits while minimizing the peak demand with four-quadrant EV chargers, since this is of particular concern for utilities [24]. A distinct aggregated EV realization is generated that comprises the aggregated daily distance traveled EVd_n, and the aggregated arrival and departure times at each node, T_n^{Arr} and T_n^{Dep}, where each of them is modeled using appropriate pdfs. An hourly $\tau_1 = 1h$ feeder control schedule and the corresponding daily peak demand value are computed using a GA-based optimization model for this realization [25], to minimize the peak demand for the day, i.e.

$$\min P^{max} = \max_{t=1,...,T_{max}} \left\{ \sum_{n=1}^{N} \left(BL_{n,t} + P_{n,t}^{ev}\right) \right\} \quad (2)$$

where all variables, parameters, and indices in this and other equations are defined in the Nomenclature. This minimizes the daily feeder peak demand, which is the maximum value of the feeder demands (sum of the EV and base loads at all the nodes) during each time interval t over the 24 h horizon. The constraints of the optimization model are the following:

- *EV Operation Constraints*: The following constraints ensure that the EV battery capacity is not exceeded, and the minimum battery SoC at the end of the charging period is SoC_n^f:

$$\sum_{t=1}^{T_{max}} P_{n,t}^{ev} \tau_1 \leq \overline{Eev_n} \quad \forall \, n = 1, ..., LN \quad (3)$$

$$\sum_{t=1}^{T_{max}} P_{n,t}^{ev} \tau_1 \geq \left(SoC_n^f - SoC_n^0\right) \overline{Eev_n} \quad \forall \, n = 1, ..., LN \quad (4)$$

$$\overline{Eev_n} = \sum_{l=1}^{nev_n} BCap_l \quad \forall \, n = 1, ..., LN \quad (5)$$

Note that, for the EV penetration levels considered in this work, constraint (4) is feasible for all generated realizations; however, this may not be the case for higher EV penetration levels. Furthermore, the limits of apparent, active, and reactive powers of aggregated four-quadrant EV loads are enforced as follows:

$$\overline{S_{n,t}^{ev}} = \sum_{l=1}^{nev_{n,t}} Mcp_l \quad \forall \, n = 1, ..., LN, \, t \quad (6)$$

$$-\overline{S_{n,t}^{ev}} \leq P_{n,t}^{ev} \leq \overline{S_{n,t}^{ev}} \quad \forall \, n = 1, ..., LN, \, t \quad (7)$$

$$-\overline{S_{n,t}^{ev}} \leq Q_{n,t}^{ev} \leq \overline{S_{n,t}^{ev}} \quad \forall \, n = 1, ..., LN, \, t \quad (8)$$

$$\left(Q_{n,t}^{ev}\right)^2 + \left(P_{n,t}^{ev}\right)^2 \leq \left(\overline{S_{n,t}^{ev}}\right)^2 \quad \forall \, n = 1, ..., LN, \, t \quad (9)$$

- *System Limits*: The physical limits of the system, i.e. the constraints on the transformer taps and switched capacitors, and the node voltage and feeder current limits, are represented as follows:

$$\underline{tap_i} \leq tap_{i,t} \leq \overline{tap_i} \quad \forall \, i, \, t \quad (10)$$

$$0 \leq cap_{j,t} \leq \overline{cap_j} \quad \forall \, j, \, t \quad (11)$$

$$\underline{V_n} \leq |V|_{n,t} \leq \overline{V}_n \quad \forall \, n = 1, ..., LN, \, t \quad (12)$$

$$\leq |I|_{b,t} \leq \overline{|I|}_b \quad \forall \, b = 1, ..., B, \, t \quad (13)$$

The apparent power limit at each node, which represents the maximum capacity of the equivalent feeder or MV/LV transformer at each node, is also considered as follows:

$$0 \leq |S|_{n,t} \leq \overline{S_{n,t}} \quad \forall \, n, \, t \quad (14)$$

- *Power Flows*: During each time interval t, the power flows are determined using OpenDSS [26], which is based on current injections and node voltages at each phase, as well as the system admittance matrix. The actual powers delivered to EV and base loads ($P_{n,t}^{ev}$ and $BL_{n,t}$), are also computed by OpenDSS, which are then used to compute the objective function value.
- *Control Operations*: The following constraints limit the number of control operations by taps and capacitors performed every hour:

$$|tap_{i,t} - tap_{i,t-1}| \leq Mop_{tap} \quad \forall \, i, \, t \qquad (15)$$

$$|cap_{j,t} - cap_{j,t-1}| \leq Mop_{cap} \quad \forall \, j, \, t \qquad (16)$$

The GA optimization technique is used here, as opposed to other optimization techniques, to solve the proposed Mixed Integer Nonlinear Programming (MINLP) problem, because GA can readily handle integer variables and is also more likely to find a solution near the global optimum, since it searches in a wider space in the feasible region and normally does not get stuck in a local minimum, which often happen with classic methods that start searching from a single initial point [27]. Thus, a comparison of the optimality gap produced for a similar MINLP formulation of the first stage, considering only EV battery smart charging using both GA and Sequential Quadratic Programming (SQP) solvers based on an integer relaxation of the original problem, is presented in [28] for an IEEE 13-bus benchmark distribution feeder. For EV penetration levels equal to or higher than 50%, the results show a lower value of the objective function for the GA solution approach compared to the relaxed version of the problem solved with an SQP solver, demonstrating that the GA method, for this MINLP problem, yields adequate results. Furthermore, this technique allows for the ready use of existing and efficient simulation packages, such as OpenDSS, to compute the power flow constraints, thus simplifying the implementation of the proposed approach.

In the Bootstrap method, K daily feeder peak demands and their corresponding discrete feeder controls, comprising of hourly tap and capacitor settings, are computed for a finite number of K realizations, using this optimization model. These independent observations populate the original sample of size K, which is then resampled to generate M Bootstrap replicates, each of size K. Consequently, the mean daily feeder peak demand $\hat{P}^{max}$ and the most likely hourly tap/capacitor settings $\hat{C}on$, are computed for the original sample, as well as for each Bootstrap sample $\hat{P}^{max*}$ and $\hat{C}on^*$. These M Bootstrap statistics are then used to obtain the sampling distributions of the desired statistics. The Bootstrap estimates of the mean feeder peak demand $E[P^{max}]$ and the most likely feeder control schedule $E[Con]$, which are the outputs of the process, are obtained by computing the mean of their respective sampling distributions, provided they approximate a normal distribution [28].

V. REAL-TIME COORDINATION OF FOUR-QUADRANT EV CHARGERS

The hourly feeder control schedule $E[Con]$ computed in the first step is used in the second step, which concentrates on the aggregated four-quadrant EV operation control performed periodically (every 5 min) at each node. The latter is implemented using an optimization approach, and the results are then compared with a popular sensitivity-based heuristic approach used in several papers (e.g. [10], [29]), and the BAU practice. All these approaches are described next.

A. Optimization Approach

In the proposed approach, the utility faces the challenge of allocating limited amount of power among all EV customers without exceeding the daily feeder peak demand, for pre-computed optimal feeder controls, and considering the perspective of EV customers. Thus, aggregate EV loads at some nodes of a radial primary distribution feeder may be at a disadvantage compared to others in the same feeder due to their locations, which affect node voltages along the feeder; hence, an increase in power to some EV loads would come at the expense of reducing power delivered to other loads. Therefore, this work focuses on a well-accepted notion of fairness in the area of telecommunications and networks, known as proportional fairness [30], which provides a balance between two competing interests, i.e. maximizing the total power delivered to the aggregate EV loads, and providing some level of power to all EV loads connected for charging. Moreover, in this model, thanks to the availability of four-quadrant EV chargers, it is possible to discharge some EV batteries and use reactive power to reduce the consumption of voltage-dependent loads to achieve the daily feeder peak demand calculated in the first stage.

Every few minutes, information is collected at each node (e.g. number of EVs, SoCs, base loads); then, an optimization problem is solved to determine how much active and reactive power each aggregate load EV would inject or absorb, assuming that everything remains constant during the 5 min period under consideration. EV active power is decomposed into positive and negative variables, i.e. P_n^{ev+} and P_n^{ev-}, which are treated as complementary variables to avoid simultaneous charging and discharging of EV batteries. Additionally, the objective function of this optimization problem contains two terms. The first term is used to maximize the charging of connected EV loads in a proportionally fair manner for each time interval for a given realization, and the second term is used to minimize the deviations with respect to the peak demand limit calculated in the first stage, as follows [31]:

$$\max \left\{ \left(\sum_{n=1}^{LN} \log \frac{P_n^{ev+}}{S_n^{ev}} \right) - \alpha \left(\sum_{n=1}^{N} \left(P_n^{ev} + P_n^{bl} \right) - E[P_{max}] \right)^2 \right\} \qquad (17)$$

where, in the first term, the ratio of P_n^{ev+} to $\overline{S_n^{ev}}$ achieves its maximum value of 1, if $P_n^{ev+} = \overline{S_n^{ev}}$; hence, by maximizing the summation of the logarithms of these ratios, this term of the objective function maximizes the power delivered to the charging EVs at each node, and provides some level of power to all nodes where there are EVs to charge. The second term is only activated, i.e. $\alpha = 1$, when the base load is larger than the

peak demand limit, meaning that at that point some EVs are required to discharge, since in this approach EV discharging is only used to avoid exceeding the peak demand limit calculated in the first step by directly feeding some neighboring loads, whereas available EV reactive power can be controlled at any moment as required by the optimization model. The use of the EV P and Q services are assumed here to be properly compensated, and are not requested unless strictly necessary, without violating the EV charging limits; thus, "standard" four-quadrant EV chargers are assumed.

The constraints of the proposed optimization model are as follows:

- *Power Flows*: OpenDSS is used here to determine the feeder flows.
- *System Limits*: The apparent power of the aggregated EVs at each node is limited by:

$$\overline{S_n^{ev}} = \sum_{l=1}^{nev_n} Mcp_l \ \ \forall \ n = 1, ..., LN \tag{18}$$

The aggregated EV active power is decomposed into a positive and negative variables, i.e. charging and discharging, as follows:

$$P_n^{ev} = P_n^{ev+} + P_n^{ev-} \ \ \forall \ n = 1, ..., LN \tag{19}$$

$$0 < P_n^{ev+} \le \overline{S_n^{ev}} \ \ \forall \ n = 1, ..., LN \tag{20}$$

$$-\overline{S_n^{ev}} \le P_n^{ev-} < 0 \ \ \forall \ n = 1, ..., LN \tag{21}$$

$$P_n^{ev-} \ P_n^{ev+} = -\epsilon \ \ \forall \ n = 1, ..., LN \tag{22}$$

$$-\overline{S_n^{ev}} \le P_n^{ev} \le \overline{S_n^{ev}} \ \ \forall \ n = 1, ..., LN \tag{23}$$

where ϵ is a small positive number. EV reactive power limits are also enforced, as follows:

$$-\overline{S_n^{ev}} \le Q_n^{ev} \le \overline{S_n^{ev}} \ \ \forall \ n = 1, ..., LN \tag{24}$$

$$(Q_n^{ev})^2 + (P_n^{ev})^2 \le \left(\overline{S_n^{ev}}\right)^2 \ \ \forall \ n = 1, ..., LN \tag{25}$$

Finally, the node voltage, feeder current, and node apparent power limits are also considered:

$$\underline{V}_n \le |V|_n \le \overline{V}_n \ \ \ \forall \ n = 1, ..., LN \tag{26}$$

$$0 \le |I|_b \le \overline{|I|}_b \ \ \ \forall \ b = 1, ..., B \tag{27}$$

$$0 \le |S|_n \le \overline{S}_n \ \ \forall \ n = 1, ..., LN \tag{28}$$

- *EV SoC*: The SoC of the individual EV batteries is calculated as follows:

$$SoC_{l,t} = SoC_{l,t-1} + \frac{P_n^{ev}\tau_2}{nev_n Mcp_l} \tag{29}$$
$$\forall \ n = 1, ..., LN, \ l = 1, ..., nev_n$$

$$SoC_{l,t} \le \overline{SoC}_l \ \ \forall \ l = 1, ..., nev_n \tag{30}$$

where the last equation guarantees that the upper limit of SoC of the EV batteries is not exceeded.

- *Peak Demand Constraint*: This constraint ensures that the total feeder load does not exceed the peak demand setpoint $E[P^{max}]$ computed in the first step, as follows:

$$\sum_{n=1}^{N} (BL_n + P_n^{ev}) \le E[P^{max}] \tag{31}$$

- *V2G Constraints*: These constraints guarantee that the second term of the objective function is only activated when the base load is larger than the peak demand limit:

$$\beta = 1 - \text{sgn}\left(\sum_{n=1}^{N} BL_n - E[P_{max}]\right) \tag{32}$$

$$\alpha \ \beta = 0, \ \ \alpha \in \{0, 1\}, \ \ \alpha \ne \beta \tag{33}$$

Note that, since at this stage the EV load is maximized every 5 minutes, the approach will ensure that EV batteries' SoCs reach a desirable level in the expected charging time considered in Stage 1, as all EV loads are allocated the maximum active power that satisfies all system constraints. Also, it should be mentioned that a GA-based solution approach is used here, since the technique used in the first step can be readily modified to solve this NLP problem, and also because OpenDSS is used to efficiently compute the power flow constraints, thus simplifying the implementation process.

B. Heuristic Approach

The sensitivity-based heuristic approach (e.g. [10], [29]) computes the active and reactive power outputs of EVs at each node from the base-case Y-bus matrix (extracted from OpenDSS), corresponding to the operating point associated with base loads in the feeder, when there are no EV loads. Thus, changes in active power load P_n and reactive power load Q_n correspond to changes in EV load ΔP_n^{ev} and ΔQ_n^{ev} at each node, which can be computed as follows:

$$\begin{bmatrix} \Delta P_n^{ev} \\ \Delta Q_n^{ev} \end{bmatrix} = J \begin{bmatrix} \Delta \delta_n \\ \Delta |V|_n \end{bmatrix} = \begin{bmatrix} \frac{\partial P_n}{\partial \delta_n} & \frac{\partial P_n}{\partial |V|_n} \\ \frac{\partial Q_n}{\partial \delta_n} & \frac{\partial Q_n}{\partial |V|_n} \end{bmatrix} \begin{bmatrix} \Delta \delta_n \\ \Delta |V|_n \end{bmatrix} \ \ \forall \ n = 1, ..., N \tag{34}$$

The base-case node voltages $|V^{bc}|_n$ are computed for the known base load at each node, which is then used to calculate the available voltage margin to the lower operating threshold as follows:

$$\Delta |V|_n = \underline{|V|}_n - |V^{bc}|_n \ \ \forall \ n = 1, ..., N \tag{35}$$

In this work, since the node voltage limits only depend on $|V|_n$, $\Delta \delta_n = 0$. Consequently, ΔP_n^{ev} and ΔQ_n^{ev} can be calculated as follows:

$$\Delta P_n^{ev} = \frac{\partial P_n}{\partial |V|_n} \ \Delta |V|_n \ \ \forall \ n = 1, ..., N \tag{36}$$

$$\Delta Q_n^{ev} = \frac{\partial Q_n}{\partial |V|_n} \ \Delta |V|_n \ \ \forall \ n = 1, ..., N \tag{37}$$

From (36), there may be load nodes where the resulting ΔP_n^{ev} exceeds the active power limit for the node; these are corrected to $\Delta P_n^{ev} = \overline{S_n^{ev}}$, if $\Delta P_n^{ev} > 0$, or $\Delta P_n^{ev} = -\overline{S_n^{ev}}$, if $\Delta P_n^{ev} < 0$. Moreover, after correcting ΔP_n^{ev}, ΔQ_n^{ev} is corrected to $\Delta Q_n^{ev} = min\{((\overline{S_n^{ev}})^2 - (\Delta P_n^{ev})^2)^{1/2}, \Delta Q_n^{ev}\}$, if $\Delta Q_n^{ev} > 0$, or $\Delta Q_n^{ev} = max\{-((\overline{S_n^{ev}})^2 - (\Delta P_n^{ev})^2)^{1/2}, \Delta Q_n^{ev}\}$, if $\Delta Q_n^{ev} < 0$. In addition, for the nodes with no EV loads, $\Delta P_n^{ev} = 0$ and $\Delta Q_n^{ev} = 0$. The corrected ΔP_n^{ev} and ΔQ_n^{ev} are then sent to OpenDSS, which computes the actual active and reactive power allocated to the EV loads at each node n every τ_2 minutes.

C. Business-as-usual

In North America, the BAU practice is to provide maximum possible power to all connected EVs, while trying to maintain node voltages within operating limits through automatic regulation of LTC taps and capacitors, and this uncontrolled operation of EVs is the reason for utility concerns regarding peak loads exceeding feeder capacities. Typically, the up or down voltage regulation using LTC taps is performed based on the node voltages at the midpoint of the feeder, i.e. if the voltage at this node is higher or lower than the maximum or minimum voltage threshold, the taps are adjusted until this node voltage is within the operating limits. This may result in frequent tap changing operations, which can decrease the lifetime of LTC taps, with large EV penetration.

VI. SIMULATION RESULTS AND DISCUSSION

A. Test System and Assumptions

The test system used in this work, depicted in Fig. 3, is a 41-node real distribution feeder extracted from [1], which is an unbalanced three-phase system with three LTC transformers controlling the secondary voltage of the transformers, which maintain the voltages of all nodes downstream from the voltage regulator within operating limits; there are no switched capacitors in this feeder. In addition, the following assumptions are made, without loss of generality:

- A 24 h time horizon is implemented, with time steps of $\tau_1 = 1$ h and $\tau_2 = 5$ min, for the day-ahead dispatch of distribution feeders and fair charging of EVs, respectively. Note that from the power system perspective, 5 min intervals would be sufficiently short for EV operation, since a finer granularity would increase voltage fluctuations, which may have detrimental effects on the lifetime of equipment and appliances serviced by the feeder.
- The hourly base load for the 24 h period is extracted from [28], and comprises of typical non-flexible residential loads, assumed known through forecasting techniques (e.g., [21]), with feeder peak demand for the day occurring at 7 pm. Table I presents the active and reactive power peak demands for all load nodes. Since this work focuses on the primary distribution feeder, all LV loads connected to the medium-voltage (MV) feeder through a distribution transformer are considered to be aggregated at a given node at the primary distribution feeder level, and are modeled as constant impedance loads.
- It is assumed that a household can have a maximum of one EV, and that the average monthly electricity consumption of a typical household in the Southern US is 1500 kWh [32]. Hence, for an EV penetration level pr, which is the percentage of total possible number of EVs on the feeder, the number of EVs at a node n is estimated as follows [1]:

$$nev_n = pr\frac{P_n^{pk}}{AHD} \quad (38)$$

where P_n^{pk} is the aggregated peak load at the node n, and the average hourly demand AHD = 1500 kWh/(24 h x 30 days). Therefore, from the peak loads provided

TABLE I
PEAK DEMAND AND NUMBER OF EVs FOR 100% PENETRATION AT DIFFERENT NODES OF REAL MV FEEDER

Node n	P_n^{pk} [kW]	Q_n^{pk} [kVar]	nev_n for 100% Penetration	Node n	P_n^{pk} [kW]	Q_n^{pk} [kVar]	nev_n for 100% Penetration
004a	2084	685	1000	014c	67	22	30
004b	2094	688	1003	022b	48	16	20
004c	2236	735	1070	023a	10	3	3
006a	301	171	143	025b	290	95	136
006b	301	171	143	027a	152	50	70
006c	301	171	143	030c	195	64	90
008a	1044	343	500	031a	171	56	80
008b	899	295	430	031b	152	50	70
008c	1245	409	596	031c	195	64	90
010a	192	169	90	034c	204	67	96
010b	192	169	90	036b	81	27	36
010c	192	169	90	037c	57	19	26
013a	6	0	2	037c	48	16	20
013b	6	0	2	041a	712	234	340
013c	6	0	2	041b	675	222	323
014a	209	69	100	041c	780	256	373
014b	71	23	33				

in Table I, the corresponding nev_n can be calculated, which would result in a total of 7240 EV loads charging from the feeder at $pr = 100\%$. The EV penetration levels considered here are 30%-60%.

- EVs are considered to operate in the V2G mode, both for active and reactive power, and modeled as constant current loads.
- In the day-ahead dispatch step, the maximum number of operating EVs, nev_n, computed based on the EV penetration level, remains constant throughout the specific charging period, T_n^{Arr} to T_n^{Dep}. In addition, the arrival and departure times of EVs are modeled as normal distributions centered around 5 pm and 7 am, and standard deviations of 2 h and 1 h [22], respectively.
- In the second step, each EV arrives and departs individually at each node; hence, each EV at node n is independent and identically distributed in terms of the arrival and departure times, and the initial battery SoC, i.e. the distribution functions from the first step are applied to each EV. Therefore, the number of EVs charging from the grid at node n for each time interval is an input measured using the communication network. In addition, only one charging window is considered during a 24 h period.
- Plug-in hybrid EV (PHEV) 30km mid-size sedans with a battery capacity of 8.14 kWh are considered as the EV loads, with Level 2 charging, i.e. up to a maximum of 4.8 kW.
- In the day-ahead dispatch of feeders, the initial battery SoC is modeled based on the daily distance traveled, which is a random variable following a lognormal distribution [23]. In the second step, this distribution function is applied to each EV load at a node to determine the vehicle's SoC. It is also assumed that only the EVs that need charging absorb active power, i.e., if the battery is fully charged, the in-built charger will be available to provide active or reactive power. Furthermore, it is also assumed that EVs will not drop out of the charging process during a given time interval t.
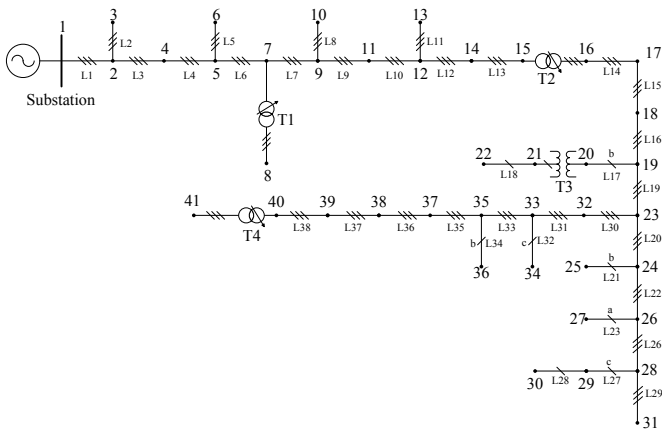
Fig. 3. 41-node real distribution feeder.

- The maximum number of tap or capacitor control operations, Mop_{tap} or Mop_{cap}, is limited to 3 per hour.
- Incentive programs are assumed to already exist, and the EV customers participation in these programs is assumed to be enforced through policy or by utilities themselves.
- The upper and lower voltage limits are assumed to be 1.1 and 0.9 p.u., respectively.

V2G can be an issue due to possible EV battery degradation; in fact, manufacturers in general do not allow this option at the present moment, although some are considering this possibility, as mentioned in [33]. Therefore, all the following four optimization scenarios are considered for comparison purposes:

- No V2G: This scenario corresponds to the normal charging mode, where EVs consume only active power.
- V2G P: In this scenario, EVs can charge or discharge the battery, without absorbing or injecting reactive power.
- V2G PQ: This scenario represents the operation of EV in all four quadrants of the PQ plane.
- V2G Q: In this scenario, EVs operate in two quadrants of the PQ plane, corresponding to positive (charging) active power, and positive and negative reactive power.

In each of these scenarios, the active and reactive power limits for EV loads, described by (7), (8), (21), and (24), are set in such a way that the operation of EVs is restricted to certain regions of the PQ plane.

B. Simulation Results

Table II presents the bootstrap mean peak demand for different penetration levels, based on 15,000 bootstrap samples generated from 25 optimization runs for each scenario and penetration level. In all penetration levels, the largest peak demand is obtained for the No V2G scenario, and the lowest is obtained either for the V2G P or the V2G PQ scenarios. The differences between the highest and lowest peak demand, for each penetration level, are found to be between 479 kW for 60% penetration, and 245 kW for 30% penetration. The reductions in peak demand compared to the No V2G scenario is due to the fact that in V2G P mode, EV batteries discharge

during the evening peak to feed neighboring loads, while in the V2G PQ scenario, EVs also reduce the node voltages by controlling reactive power, thus decreasing the base load demand. The reduction of peak demand achieved in the V2G scenarios is desirable for utilities as this reduces the need for expensive generation resources during peak demand hours.

The performance of BAU, sensitivity-based heuristic, and optimization approaches in allocating maximum possible power to the connected EVs at a 60% EV penetration level are compared in Fig. 4. Note that the optimization approach for the different scenarios performs better than the heuristic and BAU approaches for satisfying the feeder and peak demand constraints, especially during the peak hours. Observe also that the load profile obtained using the heuristic and BAU approaches violate the peak demand value $E[P^{max}]$ computed in the first step. This is because the heuristic approach is based on a linearization of the power flow equations around operating points, and thus it is effective only for a small range of voltages around the base case. Moreover, among the optimization scenarios, the No V2G scenario is able to charge the fleet of EVs faster, due to reducing the demand earlier than in the V2G P, V2G PQ, and V2G Q scenarios, as shown in Fig. 4. On the other hand, the proposed optimization technique does not violate the node voltage limits at any node in the feeder, as shown in Fig. 5, keeping the system peak below the setpoint obtained in the first step. As previously mentioned, base loads were modeled as constant impedance loads, and EVs were modeled as constant current loads, since EV batteries are charged following a constant current (CC)/constant voltage (CV) method, with the CC stage taking a large portion of the battery charging, until a cut-off point determined by the battery SoC, cell voltages, cell temperatures, or charging time is reached [34]. In both load models, the active and reactive power consumption depends on the load voltage; thus, in the case of constant impedance models, the active and reactive powers vary quadratically with respect to the load voltage, whereas for the constant current load, these vary linearly; hence, the feeders' energy consumptions depend on the load voltages. The effect of load modeling has been studied in [1], where constant impedance load and ZIP load models where compared in a residential smart charging scheme, reporting a lower energy consumption when using constant impedance models.

A particular effect of the optimization approach is the reduction in tap operations. This proposed approach uses load forecasting information, constraints the number of tap operations, and efficiently controls the active and/or reactive power of the four-quadrant EV chargers. Because of this, as seen in Table III for different EV penetration levels, the total number of tap operations is significantly lower compared to those of heuristic and BAU methods. By contrast, the heuristic and BAU methods only rely on voltage information at the secondary sides of the LTCs, maintaining these voltages within a predefined band. Figure 5 depicts the system voltages for 60% EV penetration; the dark black lines represent the node voltages at the secondary sides of LTCs, and the grey lines denote the voltages at the remaining system nodes. Note that only the BAU method presents node voltages below the accepted

TABLE II
PEAK DEMAND STATISTICS FROM FIRST STAGE FOR DIFFERENT EV PENETRATION LEVELS

Statistic (kW)	60% penetration				50% penetration			
	No V2G	V2G P	V2G PQ	V2G Q	No V2G	V2G P	V2G PQ	V2G Q
Sample mean	13477.59	12998.68	13028.56	13132.84	13368.27	13020.76	12994.39	13141.01
Bootstrap mean	13477.44	12998.70	13028.51	13132.78	13368.60	13020.93	12994.30	13140.81
Bootstrap σ	16.44	25.01	29.19	23.71	17.49	27.27	21.39	22.51
95% CI	[13445.6, 13510.45]	[12948.69, 13048.72]	[12970.12, 13086.89]	[13085.35, 13180.20]	[13335.23, 13463.01]	[12966.40, 13075.47]	[12951.53, 13037.08]	[13095.80, 13185.82]

Statistic (kW)	40% penetration				30% penetration			
	No V2G	V2G P	V2G PQ	V2G Q	No V2G	V2G P	V2G PQ	V2G Q
Sample mean	13258.73	12952.39	12986.42	13090.52	13190.02	12954.96	12944.21	13057.52
Bootstrap mean	13258.73	12952.46	12986.23	13090.49	13190.02	12954.96	12944.37	13057.57
Bootstrap σ	11.24	28.33	26.49	19.45	11.02	21.99	20.70	17.77
95% CI	[13236.78, 13280.71]	[12895.81, 13009.12]	[12933.25, 13039.22]	[13051.58, 13129.40]	[13167.98, 13211.92]	[12910.98, 12998.94]	[12902.98, 12985.77]	[13022.03, 13093.11]
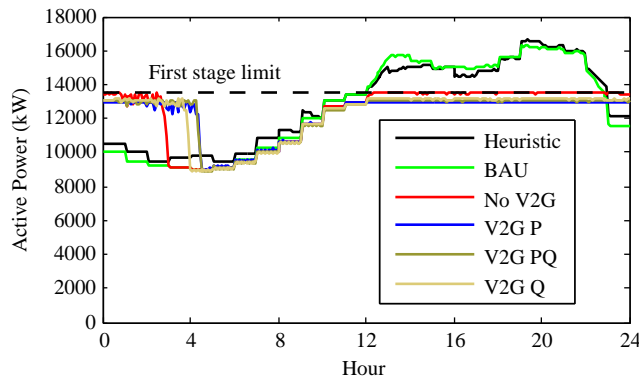
Fig. 4. Total system demand for 60% EV penetration.

TABLE III
NUMBER OF TAP OPERATIONS FOR DIFFERENT EV PENETRATION LEVELS

EV Penetration	Heuristic Method	Business as usual	No V2G	V2G P	V2G PQ	V2G Q
60%	184	337	95	88	83	80
50%	182	317	97	101	76	97
40%	187	237	103	114	83	79
30%	185	219	102	82	74	80

Fig. 5. System voltages for 60% EV penetration.

limit. Observe also that LTC secondary voltages operate in a narrow band for the heuristic and BAU approaches, compared to those for the optimization techniques. In the case of the heuristic method, all voltages are closer to 1 p.u., as EVs inject reactive power and support the voltage.

Figure 6 presents the active and reactive powers of EVs in the V2G PQ scenario for different penetration levels. Observe that power discharging is only required in the specific periods when the base load surpasses the peak demand limit calculated in the first stage, as expected; thus, the possible degradation of the batteries caused by discharging is limited. Also note that, during the discharging periods, other vehicles keep charging, but in a reduced way. Moreover, reactive power during the afternoon and evening is mostly positive, meaning that EVs are consuming reactive power to reduce voltages, and thus decrease the demand of base loads.

VII. CONCLUSIONS

This paper proposed a two-step approach for the fair operation of four-quadrant EVs, considering the primary distribution feeder characteristics and limitations, and the uncertainties associated with these loads, such as arrival and departure times, and initial battery SoCs. The proposed approach considered the utility's perspective in the first step to compute an hourly feeder control schedule that balances the total energy delivered to EVs and the risk of voltage limit violations. This was accomplished by using an optimization method and a Bootstrap technique, minimizing the feeder daily peak demand, while satisfying operational and physical limits of the feeder. In the second step, the customer's perspective was considered by allocating fair share of power to the charging EV at each load node periodically, while using the active and reactive power operation capacity of four-quadrant EV chargers to satisfy feeder limits, without exceeding the optimal peak demand setpoint obtained in the first step. The load and voltage profiles computed for a realistic distribution feeder using the proposed optimization approach show that this methodology is able to schedule four-quadrant EV loads better than a simpler heuristic
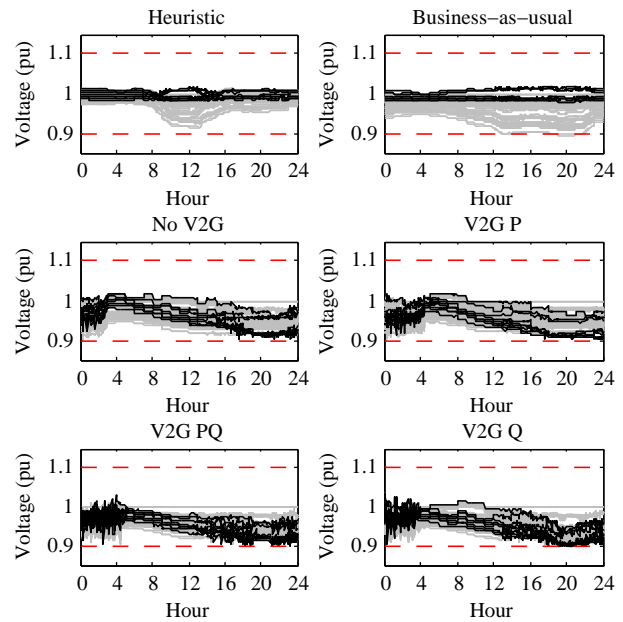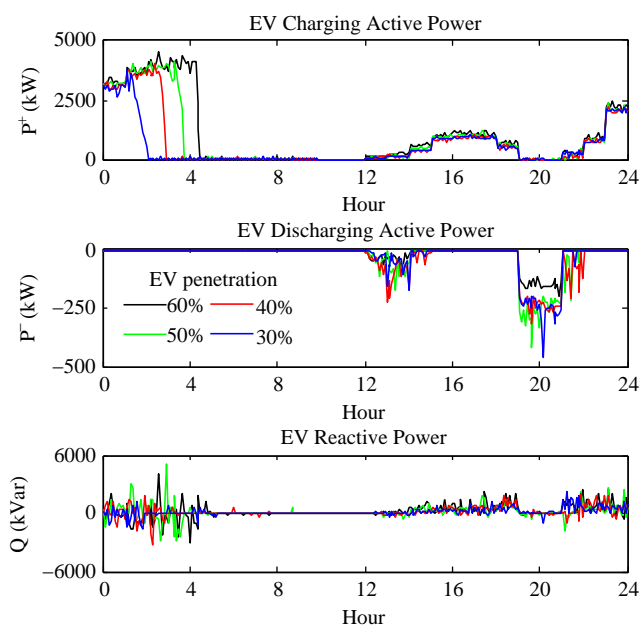
Fig. 6. Total active and reactive powers of EVs in V2G PQ scenario.

approach and the BAU practice in terms of number or taps operations, system peak demand, and voltage regulation, while satisfying feeder and peak demand constraints. Future work includes testing the performance of the proposed approach using actual four-quadrant chargers in real-time simulations for hardware-in-the-loop studies of distribution feeders and the proposed controls.

REFERENCES

[1] I. Sharma, C. Cañizares, and K. Bhattacharya, "Smart charging of PEVs penetrating into residential distribution systems," *IEEE Trans. Smart Grid*, vol. 5, no. 3, pp. 1196–1209, 2014.

[2] "Peaksaver PLUS - Consumer Programs," 2017. [Online]. Available: https://saveonenergy.ca/Consumer/Programs/Peaksaver-Plus.aspx

[3] S. Bahrami and M. Parniani, "Game theoretic based charging strategy for plug-in hybrid electric vehicles," *IEEE Trans. Smart Grid*, vol. 5, no. 5, pp. 2368–2375, Sept 2014.

[4] R. Abousleiman and R. Scholer, "Smart charging: System design and implementation for interaction between plug-in electric vehicles and the power grid," *IEEE Trans. Transport. Electrific.*, vol. PP, no. 99, pp. 1–1, 2015.

[5] N. Blaauwbroek, D. Issicaba, and J. Pecas Lopes, "Multi-agent scheme to handle flexible loads on low voltage distribution grids," in *Power Systems Computation Conference (PSCC)*, Aug 2014, pp. 1–7.

[6] O. Ardakanian, S. Keshav, and C. Rosenberg, "Real-time distributed control for smart electric vehicle chargers: From a static to a dynamic study," *IEEE Trans. Smart Grid*, vol. 5, no. 5, pp. 2295–2305, Sept 2014.

[7] A. Masoum, S. Deilami, A. Abu-Siada, and M. Masoum, "Fuzzy approach for online coordination of plug-in electric vehicle charging in smart grid," *IEEE Trans. Sustain. Energy*, vol. PP, no. 99, pp. 1–10, 2015.

[8] F. Baccino, S. Grillo, S. Massucco, and F. Silvestro, "A two-stage margin-based algorithm for optimal plug-in electric vehicles scheduling," *IEEE Trans. Smart Grid*, vol. 6, no. 2, pp. 759–766, March 2015.

[9] N. Chen, C. W. Tan, and T. Quek, "Electric vehicle charging in smart grid: Optimality and valley-filling algorithms," *IEEE J. Sel. Topics Signal Process.*, vol. 8, no. 6, pp. 1073–1083, Dec 2014.

[10] S. Deilami, A. Masoum, P. Moses, and M. Masoum, "Real-time coordination of plug-in electric vehicle charging in smart grids to minimize power losses and improve voltage profile," *IEEE Trans. Smart Grid*, vol. 2, no. 3, pp. 456–467, Sept 2011.

[11] J. de Hoog, T. Alpcan, M. Brazil, D. Thomas, and I. Mareels, "Optimal charging of electric vehicles taking distribution network constraints into account," *IEEE Trans. Power Syst.*, vol. 30, no. 1, pp. 365–375, Jan 2015.

[12] M. Manbachi, H. Farhangi, A. Palizban, and S. Arzanpour, "A novel volt-var optimization engine for smart distribution networks utilizing vehicle to grid dispatch," *International Journal of Electrical Power & Energy Systems*, vol. 74, pp. 238–251, 2016.

[13] S. Pirouzi, J. Aghaei, M. A. Latify, G. R. Yousefi, and G. Mokryani, "A robust optimization approach for active and reactive power management in smart distribution networks using electric vehicles," *IEEE Systems Journal*, 2017.

[14] M. Restrepo, C. Cañizares, and M. Kazerani, "Three-stage distribution feeder control considering four-quadrant EV chargers," *IEEE Trans. Smart Grid*, accepted December 2016.

[15] M. N. Mojdehi, M. Fardad, and P. Ghosh, "Technical and economical evaluation of reactive power service from aggregated EVs," *Electric Power Systems Research*, vol. 133, pp. 132–141, 2016.

[16] M. C. Kisacikoglu, B. Ozpineci, and L. M. Tolbert, "EV/PHEV bidirectional charger assessment for V2G reactive power operation," *IEEE Trans. Power Electron.*, vol. 28, no. 12, pp. 5717–5727, 2013.

[17] M. Yilmaz and P. T. Krein, "Review of the impact of vehicle-to-grid technologies on distribution systems and utility interfaces," *IEEE Trans. Power Electron.*, vol. 28, no. 12, pp. 5673–5689, 2013.

[18] M. Restrepo, J. Morris, M. Kazerani, and C. Canizares, "Modeling and testing of a bidirectional smart charger for distribution system EV integration," *to appear in IEEE Trans. Smart Grid*, 2016.

[19] M. Kisacikoglu, M. Kesler, and L. Tolbert, "Single-phase on-board bidirectional PEV charger for V2G reactive power operation," *IEEE Trans. Smart Grid*, vol. 6, no. 2, pp. 767–775, March 2015.

[20] H. Zhang, W. Tang, Z. Hu, Y. Song, Z. Xu, and L. Wang, "A method for forecasting the spatial and temporal distribution of PEV charging load," in *IEEE PES General Meeting*, July 2014, pp. 1–5.

[21] N. Ding, C. Benoit, G. Foggia, Y. Besanger, and F. Wurtz, "Neural network-based model design for short-term load forecast in distribution systems," *IEEE Trans. Power Syst.*, vol. PP, no. 99, pp. 1–10, 2015.

[22] T.-K. Lee, Z. Bareket, T. Gordon, and Z. Filipi, "Stochastic modeling for studies of real-world PHEV usage: Driving schedule and daily temporal distributions," *IEEE Trans. Veh. Technol.*, vol. 61, no. 4, pp. 1493–1502, May 2012.

[23] K. Qian, C. Zhou, M. Allan, and Y. Yuan, "Modeling of load demand due to EV battery charging in distribution systems," *IEEE Trans. Power Syst.*, vol. 26, no. 2, pp. 802–810, May 2011.

[24] E. Veldman and R. A. Verzijlbergh, "Distribution grid impacts of smart electric vehicle charging from different perspectives," *IEEE Trans. Smart Grid*, vol. 6, no. 1, pp. 333–342, Jan 2015.

[25] N. Mehboob, C. Canizares, and C. Rosenberg, "Day-ahead dispatch of distribution feeders considering temporal uncertainties of PEVs," in *Power Tech Conference Proceedings*, July 2015.

[26] R. Dugan, ""the open distribution system simulator™openDSS"," 2016. [Online]. Available: "https://iweb.dl.sourceforge.net/project/electricdss/OpenDSS/OpenDSSManual.pdf"

[27] S. S. Rao, *Engineering optimization: theory and practice*. John Wiley & Sons, 2009.

[28] N. Mehboob, C. Canizares, and C. Rosenberg, "Day-ahead dispatch of PEV loads in a residential distribution system," in *IEEE Power and Energy Society General Meeting*, July 2014, pp. 1–5.

[29] P. Richardson, D. Flynn, and A. Keane, "Local versus centralized charging strategies for electric vehicles in low voltage distribution systems," *IEEE Trans. Smart Grid*, vol. 3, no. 2, pp. 1020–1028, June 2012.

[30] E. Liu and K. Leung, "Proportional fair scheduling: Analytical insight under rayleigh fading environment," in *IEEE Wireless Communications and Networking Conference*, March 2008, pp. 1883–1888.

[31] D. Bertsimas, V. F. Farias, and N. Trichakis, "The price of fairness," *Operations Research*, vol. 59, no. 1, pp. 17–31, 2011. [Online]. Available: http://dx.doi.org/10.1287/opre.1100.0865

[32] "2009 Residential Energy Consumption Survey (RECS) data," Energy Information Administration, 2017. [Online]. Available: https://www.eia.gov/consumption/residential/data/2009/index.php?view=consumption#fuel-consumption

[33] D. Lauinger, F. Vuille, and D. Kuhn, "A review of the state of research on vehicle-to-grid (V2G): Progress and barriers to deployment," in *European Battery, Hybrid and Fuel Cell Electric Vehicle Congress*, 2017, pp. 1–8.

This article has been accepted for publication in a future issue of this journal, but has not been fully edited. Content may change prior to final publication. Citation information: DOI 10.1109/TSG.2018.2816404, IEEE Transactions on Smart Grid

IEEE TRANSACTIONS ON SMART GRIDS, ACCEPTED JANUARY 2018
11

[34] K. Young, C. Wang, L. Y. Wang, and K. Strunz, "Electric vehicle battery technologies," in *Electric Vehicle Integration into Modern Power Networks*. Springer, 2013, pp. 15–56.

Nafeesa Mehboob (S'11–M'17) received the B.A.Sc. degree in Electrical and Computer Engineering from the University of Windsor, Windsor, ON, Canada in 2005 and the Ph.D. degree in Electrical Engineering from the University of Waterloo, Waterloo, ON, Canada in 2016. She is currently working as a consultant for Kinectrics Inc. in Toronto, ON, Canada. She also has research and consulting experience in the automotive, building system design, and subatomic research industries in various capacities. Her research interests are in power system modeling and simulation, power system operation and control, genetic algorithms, power system optimization, grid integration of electric vehicles, energy storage systems, and distributed energy resources.

Mauricio Restrepo (S'13) received the electrical engineer and specialist in transmission and distribution systems degrees from Universidad Pontificia Bolivariana, Medellín, Colombia, in 2006 and 2010, and the Ph.D. degree in Electrical and Computer Engineering from the University of Waterloo, ON, Canada, in 2017. His research interests include electric mobility, smart grids, and simulation and optimization of power systems.

Claudio A. Cañizares (S'85-M'91-SM'00-F'07) is a Professor and the Hydro One Endowed Chair at the ECE Department of the University of Waterloo, where he has been since 1993. His highly cited research focus on modeling, simulation, computation, stability, control, and optimization issues in power and energy systems. He is a Fellow of the IEEE, the Royal Society of Canada, and the Canadian Academy of Engineering, and is the recipient of the 2017 IEEE PES Outstanding Power Engineering Educator Award, the 2016 IEEE Canada Electric Power Medal, and of other various awards and recognitions from IEEE PES Technical Committees and Working Groups.

Catherine Rosenberg (M'89–SM'96–F'11) is a Professor with the Department of Electrical and Computer Engineering at the University of Waterloo and the Canada Research Chair in the Future Internet. She is a Fellow of the Canadian Academy of Engineering. Her research interests are in networking, wireless, and energy systems. More information is available at https://ece.uwaterloo.ca/˜cath/.

Mehrdad Kazerani (S'88–M'96–SM'02) received his B.Sc., Master's and PhD degrees in Electrical Engineering from Shiraz University, Iran (1980), Concordia University, Canada (1990), and McGill University, Canada (1995), respectively. From 1982 to 1987, he was with the Energy Ministry of Iran. He is presently a Professor with the Department of Electrical and Computer Engineering, University of Waterloo, Waterloo, Ontario, Canada. He is a registered professional engineer in the province of Ontario. His research interests include current-sourced converter applications, matrix converters, distributed generation, energy storage, battery charging systems, electrified powertrains and microgrids.